ADVANCING EARTH AND SPACE SCIENCE

Earth's Future

RESEARCH ARTICLE
10.1029/2021EF002139

Key Points:

- Proxy measurements suggest that inundation of coastal stormwater networks from high water levels is common along the US Atlantic coast
- Measurements and modeling in coastal North Carolina showed stormwater network inundation at water levels within mean tidal range
- Stormwater network inundation likely increases risk of overland flooding in coastal urban areas

Supporting Information:

Supporting Information may be found in the online version of this article.

Correspondence to:

A. C. Gold,
gold@unc.edu

Citation:

Gold, A. C., Brown, C. M., Thompson, S. P., & Piehler, M. F. (2022). Inundation of stormwater infrastructure is common and increases risk of flooding in coastal urban areas along the US Atlantic coast. *Earth's Future*, *10*, e2021EF002139. https://doi.org/10.1029/2021EF002139

Received 7 APR 2021
Accepted 14 MAR 2022

Author Contributions:

Conceptualization: Adam C. Gold, Michael F. Piehler
Investigation: Adam C. Gold, Chelsea M. Brown, Suzanne P. Thompson
Methodology: Adam C. Gold, Chelsea M. Brown, Suzanne P. Thompson, Michael F. Piehler
Supervision: Michael F. Piehler
Visualization: Adam C. Gold
Writing – original draft: Adam C. Gold
Writing – review & editing: Adam C. Gold, Chelsea M. Brown, Suzanne P. Thompson, Michael F. Piehler

Inundation of Stormwater Infrastructure Is Common and Increases Risk of Flooding in Coastal Urban Areas Along the US Atlantic Coast

Adam C. Gold[1], Chelsea M. Brown[2], Suzanne P. Thompson[2], and Michael F. Piehler[1,2]

[1]Institute for the Environment, University of North Carolina at Chapel Hill, Chapel Hill, NC, USA, [2]Institute of Marine Sciences, University of North Carolina at Chapel Hill, Morehead City, NC, USA

Abstract Stormwater infrastructure can manage precipitation-driven flooding when there are no obstructions to draining. Coastal areas increasingly experience recurrent flooding due to elevated water levels from storms or tides, but the inundation of coastal stormwater infrastructure by elevated water levels has not been broadly assessed. We conservatively estimated stormwater infrastructure inundation in municipalities along the Atlantic United States coast by using areas of high-tide flooding (HTF) on roads as a proxy. We also modeled stormwater infrastructure inundation in four North Carolina municipalities and measured infrastructure inundation in one of the modeled municipalities. Combining methodologies at different scales provides context and allows the scope of stormwater infrastructure inundation to be broadly estimated. We found 137 census-designated urban areas along the Atlantic coast with road area impacted by HTF, with a median percent of total road area subject to HTF of 0.16% (IQR: 0.02%–0.53%). Based on 2010 census block data, the median number of people per urban area that live in census blocks with HTF on roads was 1,622 (IQR: 366–5,779). In total, we estimate that over 2 million people live in census blocks where HTF occurs on roadways along the US Atlantic coast. Modeling results and water level measurements indicated that extensive inundation of underground stormwater infrastructure likely occurs at water levels within the mean tidal range. These results suggest that stormwater infrastructure inundation along the US Atlantic coast is likely widespread, affects a large number of people, occurs frequently, and increases the occurrence of urban flooding.

Plain Language Summary Urban areas are often drained by underground pipes that convey stormwater runoff downstream when it rains, but coastal urban areas can experience recurrent "high-tide" flooding (HTF) that may block stormwater pipes from draining. We estimated where stormwater pipes may be influenced by recurrent flooding in urban areas along the Atlantic United States coast by finding where HTF occurs on roads. We also modeled the impacts of stormwater pipe inundation in four North Carolina municipalities and measured inundation in one of the modeled municipalities. Over 130 east coast urban areas had road area impacted by HTF and the number of people estimated to live in census blocks that had HTF on roads was more than 2 million. Modeling results and water level measurements in the four North Carolina municipalities indicated that stormwater pipes likely have reduced capacity to convey stormwater at water levels within the average tidal range. These results suggest that stormwater infrastructure inundation is common and increases the occurrence of urban flooding along the east coast of the United States.

1. Introduction

Coastal flooding is a longstanding issue which has been exacerbated by climate change (Kulp & Strauss, 2019; Nicholls et al., 1999; Wahl et al., 2015; Woodruff et al., 2013). Flooding due to extreme storm events such as hurricanes is increasing, and these extreme storms can cause massive amounts of damage to coastal communities (Hallegatte et al., 2013; Hinkel et al., 2014). While sea level rise is predicted to increase the impact of extreme storm events on coastal areas, it is also increasing the incidence of recurrent nuisance flooding known as "sunny day flooding" or "high-tide flooding" (HTF; Sweet et al., 2020, 2018). Many cities in the United States (US) already experience multiple days of HTF a year, with the number of flood days rapidly increasing (Sweet et al., 2018). During dry weather, this recurrent nuisance flooding can be disruptive to local infrastructure and economies (Hino et al., 2019; Jacobs et al., 2018). Combined with rainfall from storm events, HTF can impede stormwater drainage and result in more significant "compound" flooding (Rosenzweig et al., 2018; Shen et al., 2019; Wahl et al., 2015; Wilby, 2007).

Stormwater drainage networks aim to minimize flooding from stormwater runoff, but sea level rise threatens to reduce the efficacy (i.e., level of service) of coastal stormwater networks (Rosenzweig et al., 2018; Titus et al., 1987; Wilby, 2007). The goal of reducing precipitation-driven flooding in more developed areas has conventionally been achieved using an underground pipe network that quickly conveys stormwater runoff to a receiving waterbody using gravity (Burns et al., 2012; Hale, 2016). Older stormwater networks were designed to accommodate conditions at the time of their construction under the assumption that future conditions and variability would be similar to those in the past, but climate change has invalidated this assumption (Milly et al., 2008). Relative sea level rise in some coastal areas of the US has increased mean sea level by up to a foot since the 1960s (Eggleston & Pope, 2013; Zervas, 2009), so many coastal stormwater networks are increasingly inundated by typical high tide water levels (i.e., mean high water) or rising groundwater levels (Rotzoll & Fletcher, 2013; Sadler et al., 2020; Shen et al., 2019; Su et al., 2020; Wdowinski et al., 2016). Stormwater network inundation (also known as "tailwater condition") reduces how well the system drains during storm events (Shen et al., 2019; Wahl et al., 2015), and recurrent stormwater network inundation by saltwater also corrodes stormwater infrastructure (Bjerklie et al., 2012), promotes saltwater intrusion to groundwater (Su et al., 2020), and can mobilize fecal bacteria from co-located sanitary sewer lines (Su et al., 2020).

Inundation of underground stormwater networks has been reported in multiple cities in the US (Hino et al., 2019; Sadler et al., 2020; Shen et al., 2019; Wdowinski et al., 2016), but a broad characterization of stormwater network inundation has not been conducted. Most research on coastal urban flooding focuses on compound flooding (i.e., elevated receiving water levels combined with precipitation), but most of these studies focus on small areas or specific extreme storm events to recreate real-world flooding conditions using hydrodynamic models (Gallien et al., 2014; Hasan Tanim & Goharian, 2020; Sadler et al., 2020; Shen et al., 2019). These flooding estimates are extremely useful for the modeled study areas, but the limited spatial or temporal resolution of flooding estimates may limit their utility to identify vulnerable infrastructure hotspots at larger spatial scales or during dry-weather conditions. Instead of modeling real-world storm conditions, simple models of stormwater network inundation that calculate the stormwater network capacity at different discrete water levels may be an effective and easily scalable method to inform coastal urban flood risk. Regional- or national-scale estimates of stormwater network inundation do not exist, but these estimates, or even proxies, of stormwater network inundation would be helpful in characterizing the extent and scale of the issue. For estimates of stormwater network inundation across a large area, static inundation ("bathtub") models that use a digital elevation model (DEM) to estimate inundation at discrete water levels may serve as useful tools for managers. Static inundation models have limitations, such as over-estimating flooding extent relative to hydrodynamic models because they do not incorporate surface hydrodynamics such as friction (Castrucci & Tahvildari, 2018; Gallien et al., 2014), but their simplicity makes them well-suited for use as a diagnostic tool at large spatial scales.

In this study, we used simple proxies, static inundation models, and water level measurements to estimate stormwater network inundation at varying spatial scales. We also tested how including or excluding underground stormwater networks in static inundation modeling influences flooding estimates at high water levels and how stormwater network inundation relates to current NOAA coastal flood thresholds. Combining complementary analyses at varying spatial scales provides context and allows the scope of stormwater infrastructure to be broadly estimated despite a lack of site-specific infrastructure data. To identify locations along the Atlantic US coast where stormwater network inundation may occur, we used buffered road data from the OpenStreetMap and NOAA HTF areal extent estimates to find roads within census-designated urban areas that experience HTF, and thus likely also have subterranean inundation of the stormwater network draining the road. To characterize inundation of the stormwater network in the coastal town of Beaufort, NC, we measured water levels in stormwater infrastructure over a period of 8 months and compared them to water levels from a nearby NOAA tide gauge (Figure S1 in Supporting Information S1). We then used a static inundation model both with and without a coupled pipe network model to estimate stormwater network inundation and overland flooding across a range of water levels in Beaufort and three other cities in NC (Wilmington, Nags Head, and New Bern; Figure S1 in Supporting Information S1).

2. Materials and Methods

2.1. Case Study Areas

This study estimates HTF on roads along the US Atlantic coast, which is comprised of 15 states ranging from Florida (Atlantic coast) to Maine. We also created stormwater network inundation models for four municipalities along the North Carolina coast (Beaufort, Wilmington, New Bern, and Nags Head) and measured water levels in stormwater infrastructure in Beaufort for 8 months.

Beaufort is a small town located in coastal North Carolina on a peninsula between the mouths of the Newport and North Rivers (Figure S1 in Supporting Information S1). The downtown area of Beaufort is located directly adjacent to Taylor's Creek, a channel that receives either brackish flow from the Newport/North rivers or saline water from the Atlantic Ocean via Beaufort Inlet. Taylor's Creek has a semi-diurnal tidal with a mean range of 0.95 m (NOAA gage 8656483). The downtown area has moderate urban land use and uses conventional subsurface piping to convey stormwater from impervious surfaces directly to Taylor's Creek. The town has no stormwater backflow measures, and often documents "sunny day" HTF and compound flooding during storm events (Sweet et al., 2020). A recent survey of the stormwater network by a civil engineering firm produced measurements for most of the downtown area (shown in bold in Figure S1 in Supporting Information S1).

All four municipalities selected for the static inundation modeling have some distinct physical characteristics, but they all have all have flooding issues and large areas of development that rely on subsurface stormwater conveyance directly to a receiving waterbody. Wilmington is both the largest city and the city with highest elevation and relief. Wilmington's downtown area is directly adjacent to the Cape Fear River and has a semi-diurnal tidal with a mean range of 1.3 m above the river stage (NOAA gage 8658120), but it also has extensive suburban land use on the southern and eastern sides of the city that are affected by semi-diurnal tides from the Atlantic Ocean (NOAA gage 8658163) with a mean range of 1.21 m. New Bern is further inland and lies on the western side of the Neuse River. The Neuse River near New Bern can experience large amounts of riverine or storm surge flooding during hurricanes due to its eastward-facing orientation, and this occurred recently in 2018 during Hurricane Florence that led to damages costing hundreds of millions of dollars. Nags Head is located on the Outer Banks, east of Manteo and Roanoke Island. On its western side, Nags Head is affected by wind-driven tides within the Albemarle sound, while its eastern side is affected by semi-diurnal tides with a mean range of 0.98 m (nearby NOAA gage 8651370) from the Atlantic Ocean.

2.2. High Tide Flooding on Roads Along the US Atlantic Coast

We used publicly available national-scale road and HTF datasets to find areas where the two datasets overlapped in census-designated urban areas along the Atlantic coast of the United States. We suggest that areas where roads are inundated during HTF can act as a conservative proxy for areas where stormwater network inundation occurs during high tide events. Stormwater infrastructure is often co-located with roads (Bertsch et al., 2017), so this approach assumes roads are co-located with stormwater networks (See Section 4.3 for a discussion about methodological limitations). This estimate can be considered conservative because without stormwater network infrastructure data, we cannot estimate the extent of inundation in pipes that are underground. Therefore, the only way to estimate the incidence of underground stormwater network inundation at a national or regional scale is to detect the end results of stormwater network inundation, which is overland flooding caused by surcharge from the stormwater network or overland flooding that is actively entering the stormwater network. This assumption would likely not apply in lower-density or rural areas if there is no stormwater pipe network present, so the study focuses only on census-designated urban areas.

Census bureau urban area boundaries for 2010 were downloaded for each state from the Census Bureau website (2010 TIGER/Line® Shapefiles [census.gov]) in order to constrain the estimate to areas where the underlying assumption of the coincidence of roads and stormwater networks is likely strongest. Census block boundaries and total population estimates for 2010 were downloaded using the R package *tidycensus* (Walker & Herman, 2021). HTF areal extent estimates from NOAA were downloaded for each state (Sweet et al., 2020; https://coast.noaa.gov/slrdata/), and these estimates consist of approximately 3-m horizontal resolution raster data sets that indicate areas where "minor flooding" occurs based on a common impact threshold derived from the local tidal range: Minor flood threshold (m above MLLW) = 1.04 * (MHHW – MLLW) + 0.5; Sweet et al., 2018), where

MHHW (mean higher high water tidal datum) is the mean of the highest diurnal tide and MLLW (mean lower low water datum) is the mean of the lowest diurnal tide. Data for "driveable" roads for each state (i.e., excluding "private" roads) were downloaded from the open-source OpenStreetMap (https://www.openstreetmap.org; Barron et al., 2014) using the R package *osmextract* (Gilardi & Lovelace, 2021) on 5 September 2021. The OpenStreetMap road dataset was selected rather than the Census Bureau's TIGER dataset because the OpenStreetMap dataset explicitly identifies bridges and tunnels. Bridges and tunnels were removed from the roads dataset because including bridges and tunnels could create false positives for the inundation estimates, where the bridge or tunnel appears to overlap HTF extent when it is actually over (bridges) or under (tunnels) the inundated area; most bridges are removed from the DEMs used to calculate HTF areal extent estimates.

Processed road data consisted of GIS polylines, and a buffer was created on either side of all polylines to create polygons that approximated road surfaces. The width of the polygons were estimated multiplying the number of lanes recorded for each polyline in the OpenStreetMap dataset by 2.5 m. If no lane information was present, a two lane road was assumed, so a 5 m buffer (10 m width roadway) was generated. Waterbody outlines from the National Hydrography Dataset (NHD; i.e., ocean/sea, rivers, ponds, reservoirs) were used to remove any portions of buffered roads that intersected them to further remove false positive areas. Polygons representing buffered roads and HTF areal extent were intersected to find areas of HTF on roads. The areas of HTF on roads were then used to clip the buffered road network so that the attributes associated with the buffered road polygons could be analyzed (i.e., road type of flooded area). Areas of overlap among buffered roads where road area would be counted multiple times were extracted and dissolved to create polygons labeled simply "intersection." These intersection areas were erased from the buffered road polygon dataset to remove the overlapping polygon areas, and then the intersection areas were merged with the edited buffered road polygon dataset.

This analysis resulted in areas where HTF areal extent estimates intersect roads, assuming road width based on the number of lanes. Based on the assumptions outlined above, these data represented areas where stormwater network inundation may occur, either from surcharge of the stormwater network due to tidal flooding or from tidal flooding overtopping stormwater network inlets.

2.3. Modeling the Impacts of Tides in Stormwater Inundation in Four Case Study Cities

To complement the proxy measurement of stormwater network inundation (HTF on roads) and provide additional information about underground stormwater network capacity, we modeled the impacts of tidal water levels on stormwater network inundation in four case study cities. Stormwater network GIS data were obtained from each individual municipality by request. In total, we contacted 14 municipalities in coastal North Carolina and received data from eight municipalities. After data QC, we determined that only five municipalities had adequate data for the purpose of inundation modeling, and the main selection criteria were data coverage of the majority of the city and elevation or depth data for stormwater inverts. We chose four municipalities with good quality data: Beaufort, Wilmington, Nags Head, and New Bern. Each dataset had sporadic missing values for pipe or structure elevations, but New Bern had a large section of upland new development that was excluded due to missing survey elevations.

We then created an R package, *bathtub* (https://acgold.github.io/bathtub/), that implements a static inundation model coupled with a pipe network model to estimate stormwater network inundation at discrete water levels. The R package uses GIS data representing the stormwater network features (e.g., pipes, drop inlets, junction boxes, etc.), and creates a model object consisting of 3 simple feature objects (*sf* R package, Pebesma, 2018): "pipes," "nodes" (pipe ends), and "structures" (e.g., drop inlet, junction box, etc.). Network connectivity derived from the spatial topology is stored in the "nodes" layer. In the case of the occasional missing invert elevation at a node, the value is conservatively interpolated from nearby nodes by dropping the invert elevation a minimal amount (0.1 feet, 3 cm) from the nearest up-network value.

For the static inundation model, we used methods and source data used by NOAA to model overland inundation (SLR viewer: https://coast.noaa.gov/slr/; Marcy et al., 2011). We utilized 1/9th arcsecond (~3 m) NOAA SLR DEMs (https://coast.noaa.gov/slrdata/) and converted the vertical datum of the elevation values from NAVD88 to the local mean higher high water (MHHW) datum using a conversion raster created with the NOAA VDATUM application (https://coast.noaa.gov/htdata/Inundation/TidalSurfaces/NOAA_OCM_MHHWInterpolatedSurface.zip). For Nags Head only, the conversion factor between NAVD88 and MHHW was propagated up the stormwater

10.1029/2021EF002139

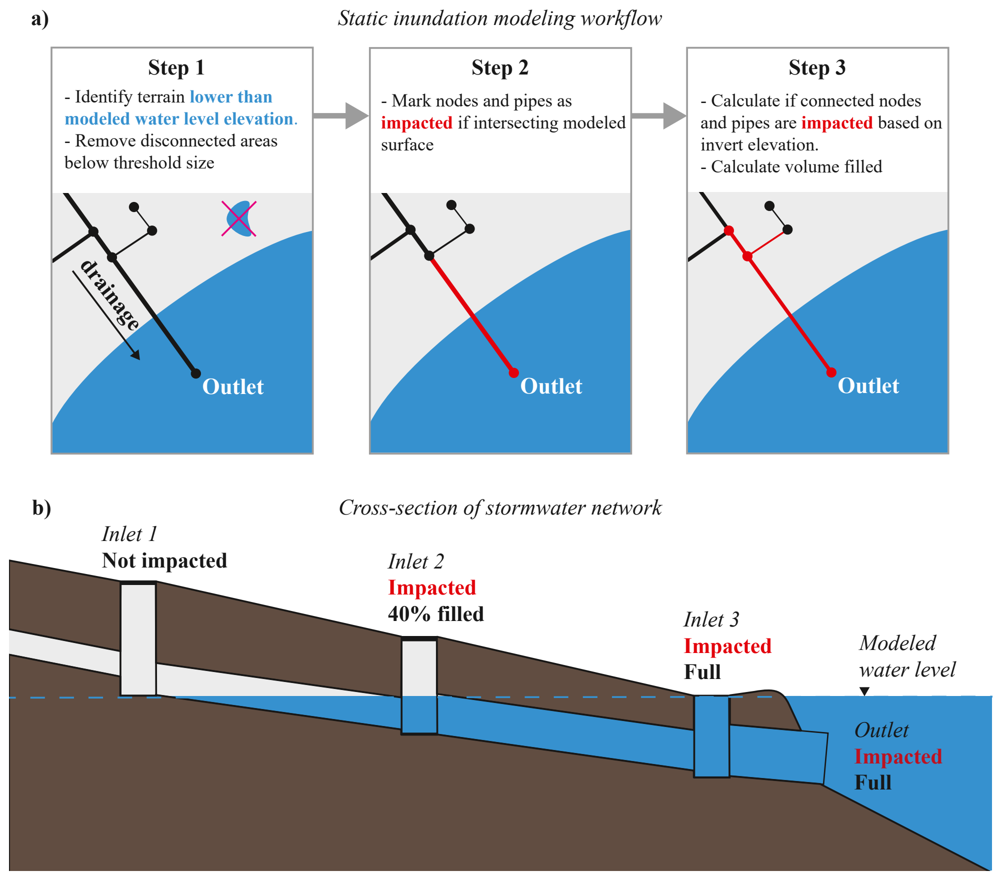

Figure 1. (a) Static inundation modeling workflow implemented in the R package *bathtub* with aerial view of an example stormwater network, and (b) a cross-section of the example in panel a that shows inundation within a stormwater network.

network because there were large differences in conversion factors between the western side (Albemarle Sound) and eastern side (Atlantic Ocean) of the barrier island. For each distinct water level modeled, areas lower than that elevation were selected, and cells were clumped to determine contiguous areas. Clumps of contiguous areas below the modeled water level elevation were filtered so that clumps smaller than a specified area (varied by study site and was constant for all model runs; Beaufort: 0.1 km^2, Nags Head: 0.3 km^2, New Bern: 0.2 km^2, Wilmington: 0.6 km^2) were removed. The minimum area threshold for each site was selected manually using an iterative process – this was necessary because study sites had different areas of extent, and clipping to the extent affected the size of modeled inundation surface clumps that represented receiving water bodies. This filtering of cells ensured that modeled inundation surface only represented areas connected to the major receiving water body and did not include isolated depressions on the landscape.

This estimate of overland flooding was used as a starting point for the pipe network model, with all nodes (pipe ends) that intersected the overland flooding extent selected and marked as "impacted" at that water level (Figure 1). The elevation of the modeled water level was propagated up-network by evaluating every node connected to the initially selected nodes by a pipe and selecting nodes with invert elevations below the specified water level (Figure 1). This propagation continued until no additional nodes were selected for the specified water level. All selected nodes and both pipes and structures connected to them were marked as "impacted," and using the diameter of each pipe end and the depth of each structure, the percent inundation of each object (i.e., nodes and structures) was calculated (Figure 1). If the diameter of the pipe end was not known, the percent inundation was marked as "unknown".

Error estimates for model results were calculated using the z-score mapping method (Schmid et al., 2014), which produces a p-value that indicates the likelihood of inundation at a particular water level for each DEM pixel or stormwater network component. For the static inundation model, error estimates incorporated the root mean squared error (RMSE) of the source DEM and the error associated with converting elevations from NAVD88 to MHHW. For this study, vertical RMSE of the source NOAA DEM was assumed 20 cm (actual RMSE is no more than 18.5 cm, NOAA, 2017) while vertical RMSE of the conversion factor from NAVD88 to MHHW, which can range from "several centimeters to tens of centimeters depending on location" (NOAA, 2017), was estimated as 10 cm. In computing z-scores for stormwater network components, the measurement vertical RMSE of network invert elevations was estimated as 20 cm (a conservative vertical RMSE for surveying GPS units) and was added to the error components from the static inundation model if invert elevations were derived from depth measurements. If invert elevations were directly measured, only the measurement error and the conversion error between NAVD88 and MHHW were combined for uncertainty calculations. P-values derived from z-scores allowed for predicted impacted infrastructure to be classified as "high confidence" (80% confidence, $p < 0.2$) or "low confidence" (20% confidence, $p < 0.8$) following methods used by the NOAA sea level rise viewer (Marcy et al., 2011; Schmid et al., 2014).

Using the *bathtub* R package, we modeled inundation in all four study cities between the water levels of −1 and 1 m MHHW by 10 cm increments. To estimate flooding caused by stormwater network surcharge, the number of inlet structures impacted at each water level estimated by the model that incorporated the stormwater network were compared to the number of inlet structures impacted by the model that did not incorporate the stormwater network.

2.4. Monitoring Water Level in Beaufort, NC

To provide evidence of stormwater network inundation, we monitored water level in select stormwater infrastructure in Beaufort, NC. Two stormwater outfalls were selected for water level monitoring (Figure S1 in Supporting Information S1, OS-outfall and MP-outfall), and water level within the pipes was measured every 30 min from June 2017 to February 2018 (8 months) using a Teledyne ISCO 750 low-profile area velocity flow sensor, which uses a pressure transducer for level and a acoustic doppler sensor for velocity. In late November (for 3 months), we began measuring water level in a storm drain upstream from the MP site (Figure S1 in Supporting Information S1, MP-upstream).

To compare our measured water levels with water levels estimated using a static inundation modeling approach, water level data from a NOAA water level gauge located in Beaufort on Taylor's Creek were downloaded. Using a static inundation modeling approach, the water level in each monitored infrastructure site was calculated using the elevation of the NOAA water level and the surveyed invert elevations of our monitored sites (NAVD88). Pipe diameter measurements for the two monitored outfalls and one storm drain were used to calculate the percent cross-sectional area inundated at the pipe ends for each time step of measured and estimated water level.

3. Results

3.1. High Tide Flooding on Roads Along the US Atlantic Coast

HTF on roads was estimated to occur to some extent in 137 census-designated urban areas along the US Atlantic coast, indicating that inundation of stormwater infrastructure may occur in many of these municipalities during high tide unless backflow measures exist (Figure 2). The metro areas of Miami, FL, New York City, NY, and Boston, MA had the largest estimated extent of HTF on roads, partially because of the overall large amount of roads (Figures 2a and 2b, See Figure 3 for Miami example). The majority of estimated impacted roads are classified as residential or service roads (e.g., parking lots, alleys, etc.), but larger and higher-traffic roads (tertiary – trunk) were also estimated to be impacted in larger metro areas (Figures 2b and 2c).

We found that the relative impact of HTF on roads varied greatly between municipalities, ranging from just over 0%–37.4% of total road area impacted by HTF (Figure 4). Although most urban areas had relatively small amounts of total road area impacted by HTF (median = 0.16%, IQR = 0.02% – 0.53%, Figure 4b), this estimated HTF on roads likely impacts a large number of people living in these areas (Figure 4c). Based on 2010 census data, a median population of 1,622 per urban area live in census blocks impacted by HTF on roads (IQR = 366–5,779; Figure 3c). In some larger urban areas, such as New York, Miami, or Boston, the estimated number of people living in census blocks impacted by HTF on roads exceeded thousands to hundreds of thousands of people. In total, we estimate that 2,059,234 people live in census blocks where HTF occurs on roads along the US Atlantic

10.1029/2021EF002139

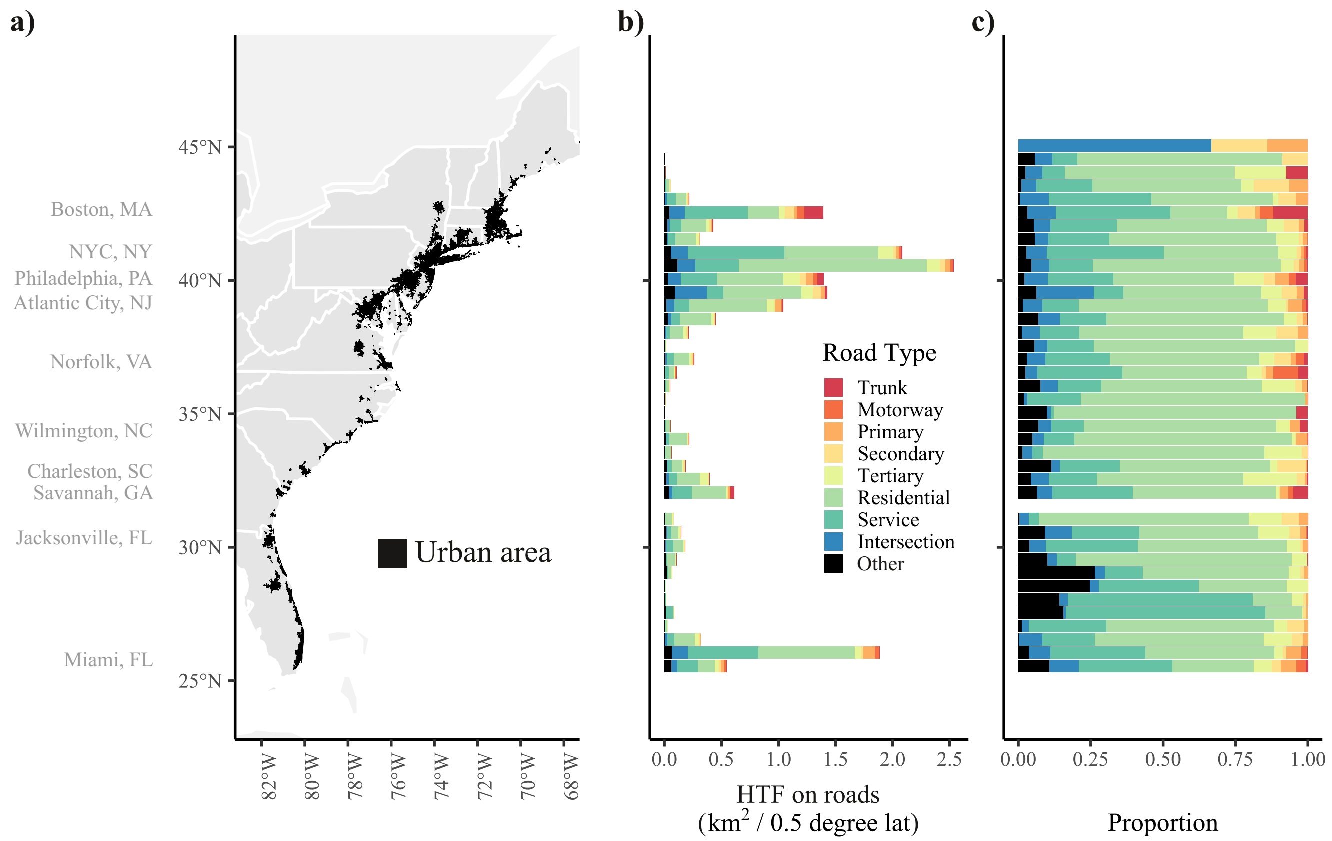

Figure 2. Area of HTF on city roads. (a) Map of 2010 census-designated urban areas along the US Atlantic coast, (b) road area overlapping estimated HTF extent binned by 0.5° of latitude, and (c) proportion of impacted road area separated by road type.

coast. The urban areas did not align with the boundaries of the municipalities measured or modeled in this study, but of the corresponding urban areas Morehead City (including Beaufort) had the highest percent of total road area impacted by HTF (0.53%, 11,446 people), followed by Wilmington (0.39%, 21,349 people), Nags Head (0.26%, 6,143 people), and New Bern (0.02%, 2,443 people).

3.2. Modeling the Impacts of Tides in Stormwater Inundation in Four Case Study Cities

Modeling the impacts of a range of water levels on stormwater infrastructure inundation for the Town of Beaufort showed that the stormwater network likely has extensive inundation at water levels within the average tidal range (mean sea level = −0.557 m MHHW, mean high water = −0.087 m MHHW; Figure 5a). At lower water levels, the inundation estimates are completely subsurface (Figure 5a), but beginning around 0.4–0.5 m MHHW (lower than the NOAA HTF threshold), portions of the stormwater network reach full capacity and result in surcharging and ponding on roadways (Figure 5, Figure S2 in Supporting Information S1). Model simulations that do not incorporate conveyance via the stormwater network show overland flooding due to shoreline overtopping at 0.7 m MHHW (Figure S2 in Supporting Information S1), and the estimated number of stormwater inlets impacted by solely overland flooding ("Excluding stormwater network" line in Figure 5a) is consistently smaller than the estimated number of inlets that are at full capacity (Figure 5a).

Inundation modeling in Wilmington, New Bern, and Nags Head showed that stormwater network inundation likely also occurs often in these cities at typical water levels, but the percent of infrastructure impacted is lower than in Beaufort (Figure 5 – note the different vertical scales for each municipality). As in Beaufort, all of the study cities had extensive estimated subsurface inundation at water levels within the average tidal range, and most estimated inundation did not result in overland flooding (Figure 5). Comparing model simulations that incorporate the stormwater network with model simulations that exclude the stormwater network showed that estimates of stormwater inlet surcharge in Wilmington and New Bern aligned well. Similar to Beaufort, though,

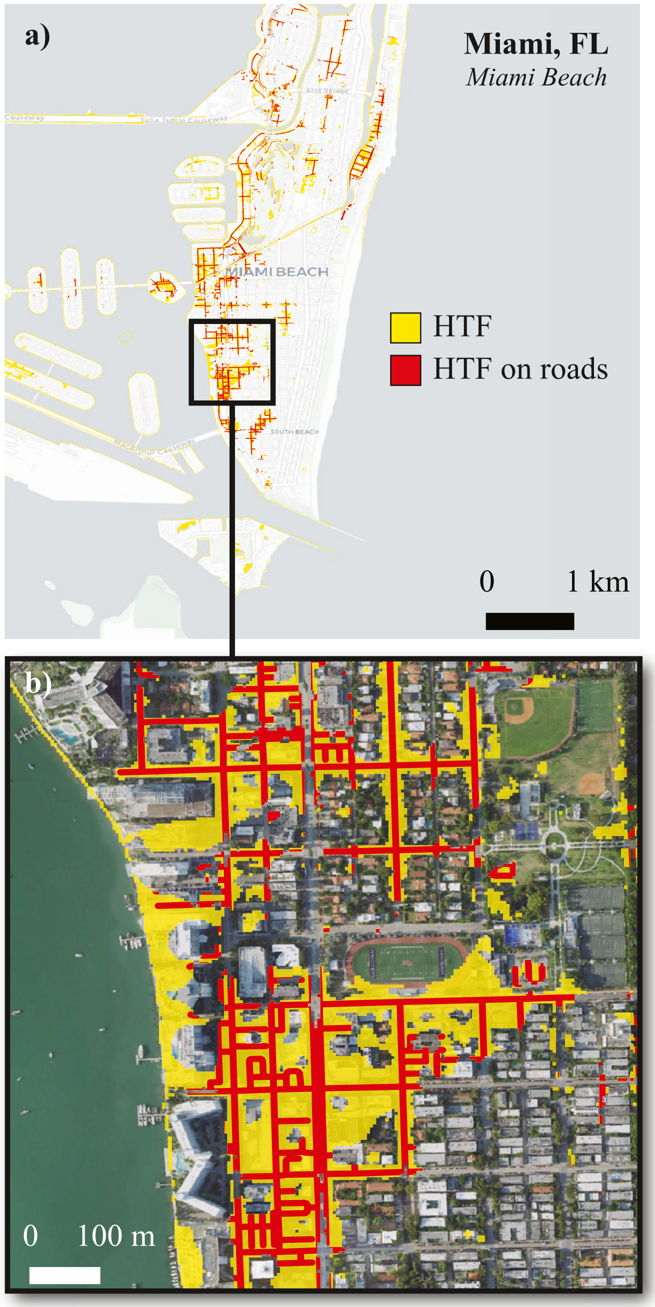

Figure 3. Example of HTF and HTF on roads for Miami beach.

the estimated number of fully inundated (i.e., "full" in Figure 5) structures in Nags Head as estimated by model simulations that incorporate the stormwater network was much higher than predicted by flooding estimates that do not incorporate the stormwater network (Figure 5).

3.3. Monitoring Water Level in Beaufort, NC

In Beaufort, NC, the two monitored stormwater outfalls experienced some degree of tidal inundation every tidal cycle throughout the 8-month monitoring period (data shown for December 2017 in Figure 6). The upstream monitored storm drain (MP-upstream) was located more than 200 m up-network from the corresponding outfall

10.1029/2021EF002139

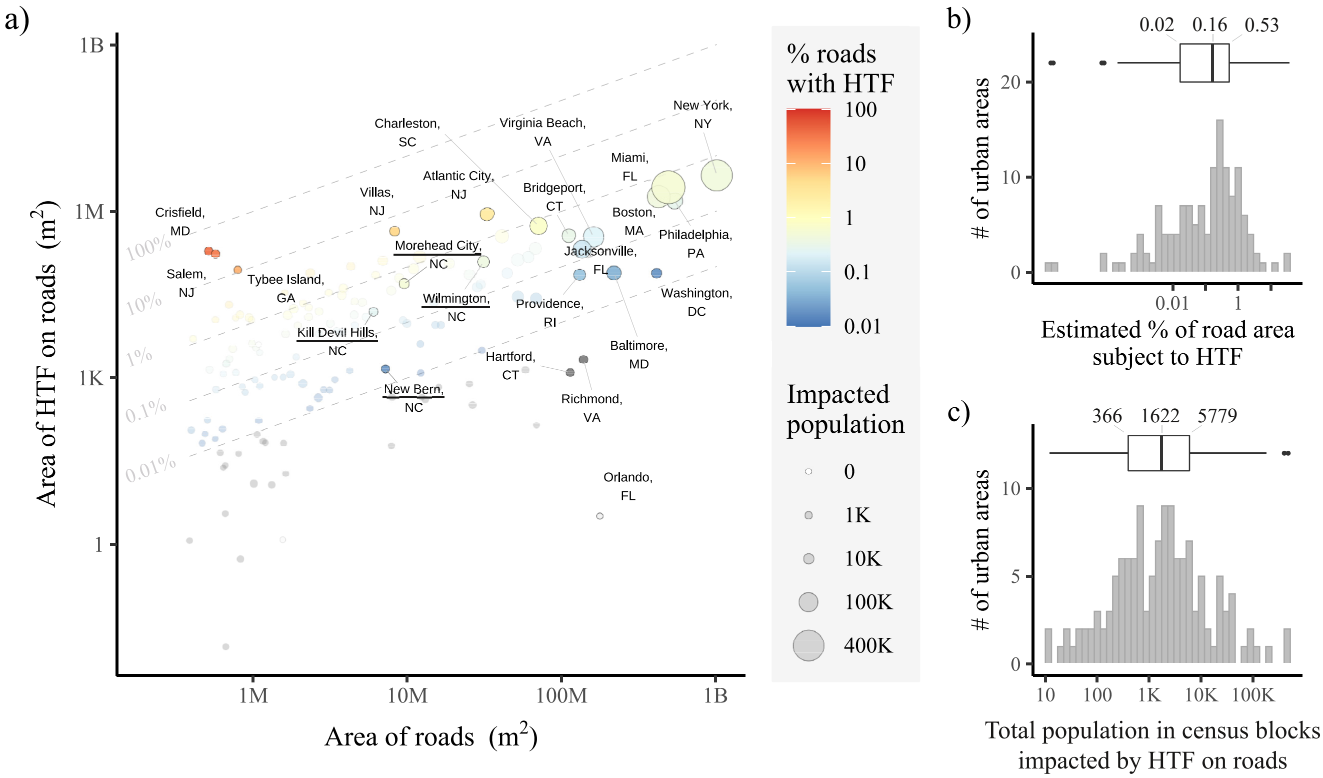

Figure 4. (a) HTF on roads compared to total road area for urban areas along the US Atlantic coast that experience some degree of HTF. Dotted lines and color indicate the estimated percent of road area subject to HTF in each urban area. Point size indicates the estimated population that lives in census blocks in the urban area that are impacted by HTF on roads. Selected municipalities are labeled, including urban areas that contain the four study municipalities which are underlined (Beaufort, Nags Head, New Bern, and Wilmington, NC). (b) Histogram of percent of total road area impacted by HTF. (c) Histogram of estimated population in each urban area that live in census blocks that have HTF on roads.

(MP-outfall), but MP-upstream also experienced significant tidal inundation during more extreme high-tide events (Figure 6). Water level in each monitored outfall was predicted based on NOAA water level from a nearby gauge and the invert elevation of the infrastructure. Predicted water level measurements corresponded well with observed water levels ($r^2 = 0.72$–0.95), as did cumulative distribution functions of predicted and observed pipe inundation percent (Figure S3 in Supporting Information S1). The predicted water levels for the MP-upstream site were slightly higher than the measured water levels, and the predicted cumulative distribution of inundation percent over-predicted the occurrence of small amounts of inundation in the storm drain (Figure S3 in Supporting Information S1).

4. Discussion

Inundation of stormwater infrastructure can have a large local impact on the frequency and magnitude of urban flooding, but this phenomenon remains difficult to characterize. Using national HTF and road data, this study demonstrated that tidal inundation on coastal roads, and thus stormwater infrastructure, likely occurs in municipalities along the Atlantic coast of the United States. Although the relative impact of HTF on the total road network was low for many of the urban areas analyzed, we estimate that over 2 million people live in census blocks along the US Atlantic coast that experience HTF on roads. These estimates of HTF on roads and the number of people impacted shows the scale at which tidal inundation of stormwater networks may impair drainage and contribute to increased incidence of flooding and the US Atlantic coast.

Using a static inundation model coupled with a stormwater network model (see Methods), we found that all four study municipalities likely experience frequent inundation of underground stormwater infrastructure that impairs their ability to convey stormwater. Inundation of the underground stormwater network occurred at water levels far below local NOAA "minor flooding" thresholds (~0.53 m above MHHW), suggesting that current and future

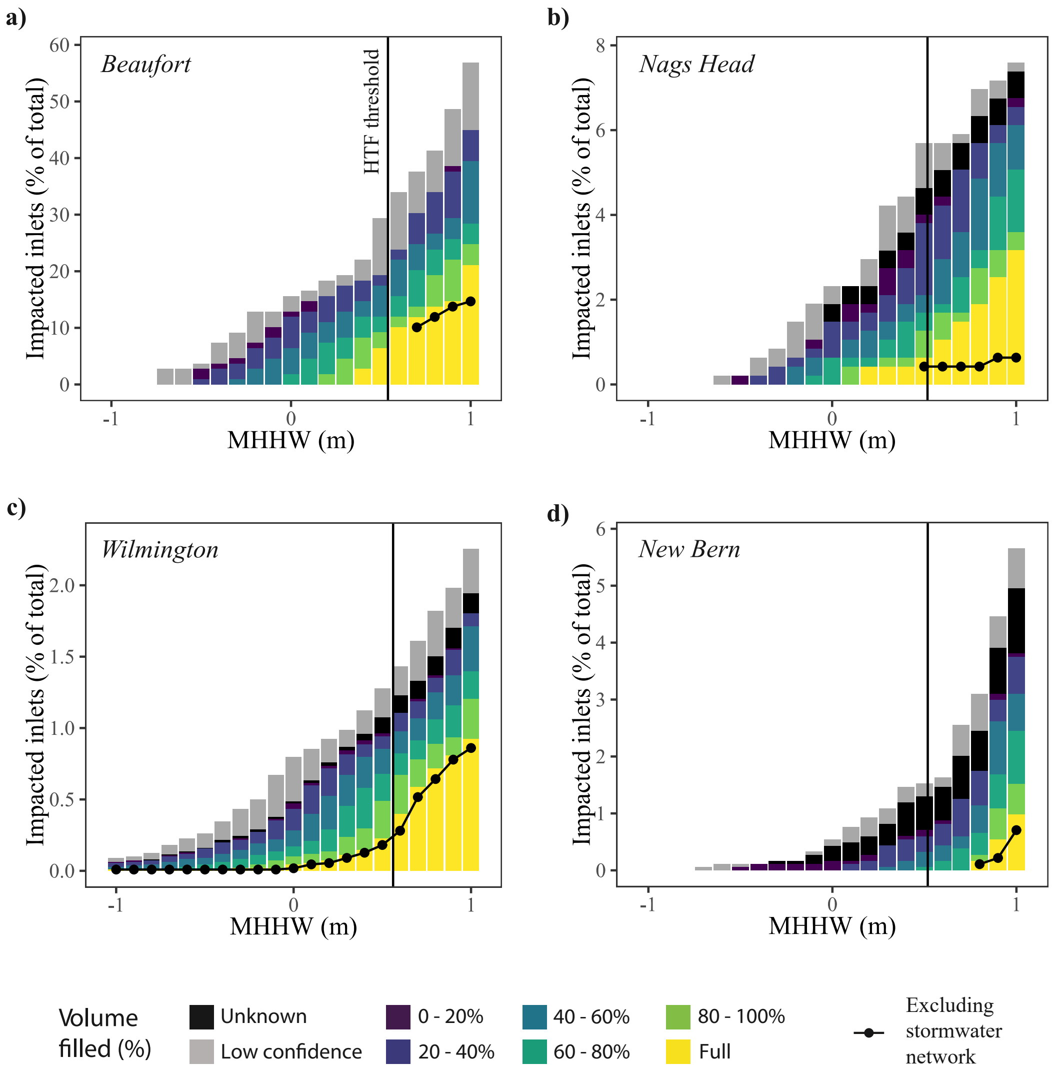

Figure 5. Percent of all modeled stormwater inlets that are impacted in (a) Beaufort, (b) Nags Head, (c) Wilmington, (d) and New Bern, NC across a range of water levels modeled with (stacked bars) and excluding (black dots/line) the stormwater network. NOAA HTF threshold from tide gage (or estimated threshold for Nags Head and New Bern) is shown as a black vertical bar.

estimates of HTF extent and frequency may underestimate urban flood risk due to reduced stormwater capacity. Stormwater network inundation below the NOAA HTF threshold also suggests that using HTF on roads as a proxy for stormwater network inundation is conservative and likely underestimates the extent of stormwater network inundation. While stormwater networks aim to drain stormwater runoff, model results from Beaufort and Nags Head showed that the stormwater networks can act as a conduit for elevated downstream waters to flood low-lying inland areas that would otherwise be disconnected from receiving waters.

Measuring stormwater infrastructure inundation at a local scale in Beaufort, NC to help validate modeling results showed that gauged stormwater outfalls were inundated by the tide daily, and the monitored upstream storm drain was inundated during extreme high tides. Predictions of pipe water level based on local NOAA water level data and pipe elevations showed that predicted outfall water levels corresponded well with measured water levels, but predicted water levels for the upstream storm drain were slightly higher than measured water levels, highlighting an acknowledged weakness of static inundation models.

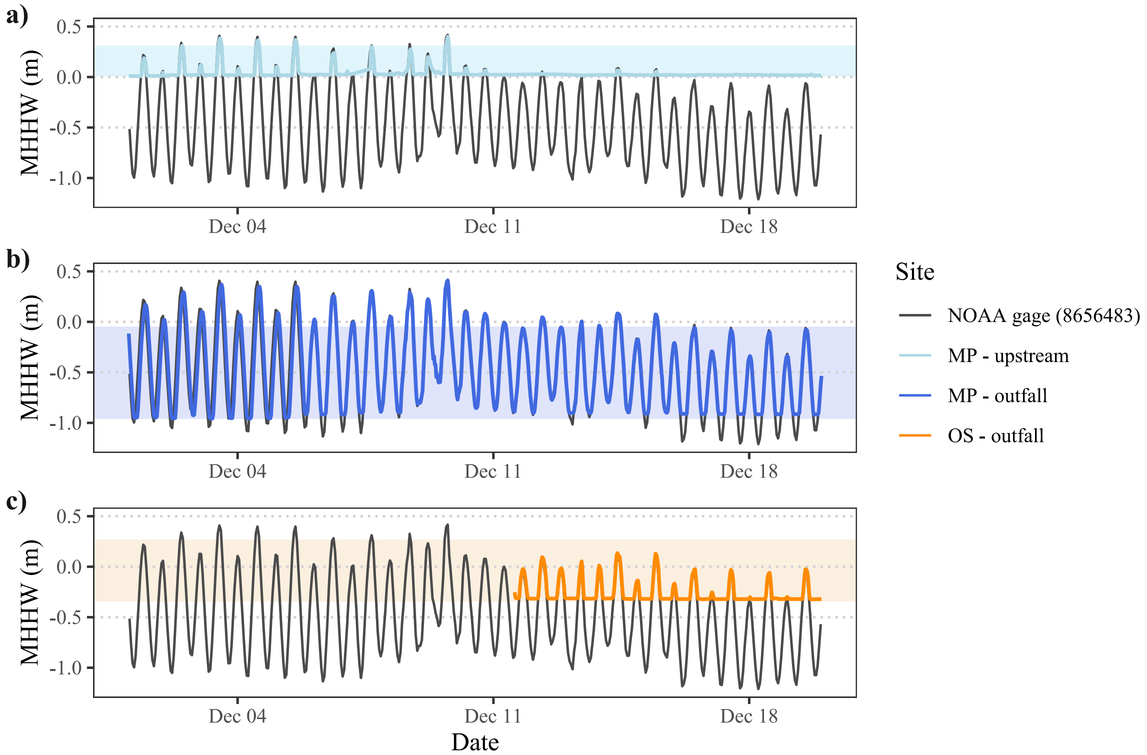

Figure 6. Snapshot of measured water levels in pipes. Example of water level measured in selected pipes (color lines) and a NOAA tide gage in Beaufort, NC (gray line) in December 2017. Shaded areas represent the dimensions of the pipe, showing that the monitored pipes were frequently filled with water from the receiving water body. Water level from OS – outfall (panel c) is missing on the graph prior to Dec 11 due to equipment malfunction.

4.1. Impacts of Network Inundation

The measured and estimated stormwater network inundation in this study demonstrate that stormwater network inundation can occur at water levels within the current average tidal range and can lead to a decrease in stormwater network capacity. It is well-known that elevated water levels are a major driver of coastal urban flooding during extreme storm events such as hurricanes (Shen et al., 2019), but this study further shows that some stormwater networks may have reduced capacity to convey runoff during typical storm conditions and water levels within the average tidal range that are far below local NOAA "minor flooding" thresholds frequently used to characterize HTF (e.g., Sweet et al., 2018). Storm surge is likely not required to impair stormwater network drainage; current mean high water levels could affect stormwater network capacity even absent overland flooding due to tides.

Inundation estimates of infrastructure in the study cities, especially Beaufort and Nags Head, also suggest that the stormwater network may act as conduit for receiving waters to flood low-lying areas at high water levels. While predicting the occurrence of this phenomenon requires detailed stormwater network information, the estimates of total road area impacted by HTF for the urban areas that contain Beaufort and Nags Head (0.53% and 0.26%, respectively, Figure 3a) suggest that this specific phenomenon likely occurs elsewhere along the US Atlantic coast. This overland flooding that is counterintuitively exacerbated by stormwater networks could have negative impacts during both dry and wet weather. During dry weather, this overland "nuisance" flooding could have negative economic impacts for local businesses by limiting access (Hino et al., 2019) or increasing traffic and travel times (Kasmalkar et al., 2020; Praharaj et al., 2021). During wet weather, this overland flooding would effectively reduce the ability of the surrounding area to drain, depending on the amount and intensity of precipitation. An example of this HTF via the stormwater network is evident in Beaufort, where a section of road adjacent to Taylor's Creek (Front St.) is predicted to flood at 0.4–0.5 m MHHW (Figure S2 in Supporting Information S1). These model results align with high tide flood reports at this location (Figure S4 in Supporting Information S1) and NOAA estimates of HTF during dry weather (https://bit.ly/30MWUGi).

During dry weather, the inundation of subsurface pipes with brackish or saltwater at water levels within the average tidal range can degrade them (Bjerklie et al., 2012) and promote saltwater intrusion and the transmission of fecal bacteria from nearby sewer lines (Su et al., 2020). We did not directly measure or model either of these effects, but during water level data collection in Beaufort, we did find qualitative evidence of network degradation in the form of oysters and barnacles growing within the stormwater network or cracked pipes (Figures S5–S7 in Supporting Information S1). The issue of stormwater and sanitary sewer degradation from inundation likely exists in Beaufort, as a previous study in the area measured high levels of human-sourced fecal indicator bacteria in piped stormwater runoff (Parker et al., 2010).

4.2. Addressing Network Inundation in the Short- and Long-Term

The threat of coastal flooding is increasing due to rising seas and the effects of climate change on precipitation patterns (Kulp & Strauss, 2019; Nicholls et al., 1999; Sweet et al., 2018, 2020; Wahl et al., 2015; Woodruff et al., 2013), and many low-lying coastal areas will need to adapt quickly to both increased stormwater network inundation and excessive stormwater runoff.

For stormwater network inundation in the short term, the most direct engineering solution is to install tide gates that prevent flow up-network when receiving water levels are elevated. These tide gates reduce tidal inundation (Sadler et al., 2020; Shen et al., 2019), including efforts to make these tide gates responsive to current and predicted inundation to increase their efficacy (Sadler et al., 2020). Though this retrofit to the current stormwater network may be effective in the short-to medium-term, predicted increases in sea level and groundwater will inevitably lead to continuously inundated outfalls in vulnerable locations and decreased surface storage of stormwater further inland (Davtalab et al., 2020; Rotzoll & Fletcher, 2013).

Addressing the long-term issue of coastal urban flooding, which includes both stormwater network inundation and excess stormwater runoff volumes, will require substantial investment in planning and upgrading drainage systems (Wilby & Keenan, 2012). A discussion of this broader adaptation and planning effort is outside the scope of the current study, but these strategies broadly include updating infrastructure to address network inundation (e.g., backflow prevention, pumping), decentralized or low impact development to manage stormwater (e.g., stormwater harvesting), landscape-scale planning to incorporate surface storage of flood waters, and possibly managed retreat or buyouts of vulnerable areas (Rogers et al., 2020; Rosenzweig et al., 2018; Wilby & Keenan, 2012).

4.3. Limitations

This study uses proxy indices and simple models to quantify the issue of stormwater network inundation due to elevated water levels along the US Atlantic coast. The methods used rely on various assumptions, so the results of this study should be interpreted in the context of the methodological limitations. First, the spatial analysis of HTF on roads in urban areas along the US Atlantic coast was assumed to indicate potential stormwater network inundation. While stormwater networks and roads are often co-located (Bertsch et al., 2017), the assumed link between HTF on roads and stormwater network inundation has not been validated. Due to lack of local infrastructure data, this assumption also ignores local infrastructure details that could mediate stormwater network inundation, such as the existence of any backflow prevention measures in the stormwater network infrastructure that could invalidate the link between HTF on roads and stormwater network inundation. The relationship between HTF on roads and stormwater network inundation would be an important assumption to validate that would increase the utility of the results and inform an interpretation of uncertainty for this metric. Second, the spatial analysis of HTF on roads utilized OpenStreetMap data and used an assumption of road width based on the number of lanes provided in the OpenStreetMap dataset. OpenStreetMap is a crowd-sourced dataset that can change over time with user input, and it does not undergo the same quality control as, for example, the Census Bureau TIGER dataset. The road width estimation (road width = 2.5 m * # of lanes) allows for more accurate representation than a fixed road width for all road types, but likely differ from real-world road widths given spatial variability in road conditions. Finally, this study focuses on dry conditions, models static water levels, and makes inferences about stormwater network capacity during potential storm event conditions. Modeling considers storm events by incorporating hydrodynamics and surface flow would more accurately estimate flooding conditions than the methods used here, but this study represents an effort to characterize the scale of the issue of stormwater network inundation across large spatial scales.

5. Conclusions

Overall, this study shows that stormwater network inundation in urban areas along the US Atlantic coast is likely widespread, affects a large number of people, occurs often, and increases the occurrence of flooding. The combination of simple modeling and measurements of stormwater network inundation at varying spatial scales used in this study provides a unique and promising approach to identify vulnerable stormwater infrastructure, but future investigation is needed to further characterize the extent of coastal stormwater network inundation to inform planning efforts. The simple modeling framework presented here can be used as an initial step for both municipalities and researchers to identify vulnerable infrastructure.

Data Availability Statement

Data and code used in the analyses are freely available on GitHub (https://github.com/acgold/HTF-on-roads) and Zenodo.org (https://doi.org/10.5281/zenodo.5562568).

Acknowledgments

We thank two anonymous reviewers as well as Drs. Miyuki Hino and Katherine Anarde for offering comments on previous versions of the manuscript. This research was supported by The National Science Foundation Growing Convergent Research Program, National Oceanographic and Atmospheric Administration National Estuarine Research Reserve System Science Collaborative, and the North Carolina Policy Collaboratory.

References

Barron, C., Neis, P., & Zipf, A. (2014). A comprehensive framework for intrinsic OpenStreetMap quality analysis. *Transactions in GIS*, *18*(6), 877–895. https://doi.org/10.1111/tgis.12073

Bertsch, R., Glenis, V., & Kilsby, C. (2017). Urban flood simulation using synthetic storm drain networks. *Water (Switzerland)*, *9*(12), 925. https://doi.org/10.3390/w9120925

Bjerklie, D. M., Mullaney, J. R., Stone, J. R., Skinner, B. J., & Ramlow, M. A. (2012). *Preliminary investigation of the effects of sea-level rise on groundwater levels in New Haven, Connecticut*. Retrieved from https://pubs.usgs.gov/of/2012/1025/pdf/ofr2012-1025_report_508.pdf

Burns, M. J., Fletcher, T. D., Walsh, C. J., Ladson, A. R., & Hatt, B. E. (2012). Hydrologic shortcomings of conventional urban stormwater management and opportunities for reform. *Landscape and Urban Planning*, *105*(3), 230–240. https://doi.org/10.1016/j.landurbplan.2011.12.012

Castrucci, L., & Tahvildari, N. (2018). Modeling the impacts of sea level rise on storm surge inundation in flood-prone urban areas of Hampton roads, Virginia. *Marine Technology Society Journal*, *52*(2), 92–105. https://doi.org/10.4031/MTSJ.52.2.11

Davtalab, R., Mirchi, A., Harris, R. J., Troilo, M. X., & Madani, K. (2020). Sea level rise effect on groundwater rise and stormwater retention pond reliability. *Water*, *12*(4), 1129. https://doi.org/10.3390/w12041129

Eggleston, J., & Pope, J. (2013). *Land subsidence and relative sea-level rise in the southern Chesapeake Bay region*. USGS Circular.

Gallien, T. W., Sanders, B. F., & Flick, R. E. (2014). Urban coastal flood prediction: Integrating wave overtopping, flood defenses and drainage. *Coastal Engineering*, *91*, 18–28. https://doi.org/10.1016/j.coastaleng.2014.04.007

Gilardi, A., & Lovelace, R. (2021). *osmextract: Download and import Open StreetMap data extracts*. Retrieved from https://CRAN.R-project.org/package=osmextract

Hale, R. L. (2016). Spatial and temporal variation in local stormwater infrastructure use and stormwater management paradigms over the 20th century. *Water (Switzerland)*, *8*(7), 310. https://doi.org/10.3390/w8070310

Hallegatte, S., Green, C., Nicholls, R. J., & Corfee-Morlot, J. (2013). Future flood losses in major coastal cities. *Nature Climate Change*, *3*(9), 802–806. https://doi.org/10.1038/nclimate1979

Hasan Tanim, A., & Goharian, E. (2020). Developing a hybrid modeling and multivariate analysis framework for storm surge and runoff interactions in urban coastal flooding. *Journal of Hydrology*, *595*(October), 125670. https://doi.org/10.1016/j.jhydrol.2020.125670

Hinkel, J., Lincke, D., Vafeidis, A. T., Perrette, M., Nicholls, R. J., Tol, R. S. J., et al. (2014). Coastal flood damage and adaptation costs under 21st century sea-level rise. *Proceedings of the National Academy of Sciences of the United States of America*, *111*(9), 3292–3297. https://doi.org/10.1073/pnas.1222469111

Hino, M., Belanger, S. T., Field, C. B., Davies, A. R., & Mach, K. J. (2019). High-tide flooding disrupts local economic activity. *Science Advances*, *5*(2), 1–10. https://doi.org/10.1126/sciadv.aau2736

Jacobs, J. M., Cattaneo, L. R., Sweet, W., & Mansfield, T. (2018). Recent and future outlooks for nuisance flooding impacts on roadways on the U.S. East Coast. *Transportation Research Record*, *2672*(2), 1–10. https://doi.org/10.1177/0361198118756366

Kasmalkar, I. G., Serafin, K. A., Miao, Y., Bick, I. A., Ortolano, L., Ouyang, D., & Suckale, J. (2020). When floods hit the road: Resilience to flood-related traffic disruption in the San Francisco Bay Area and beyond. *Science Advances*, *6*(32), 1–9. https://doi.org/10.1126/sciadv.aba2423

Kulp, S. A., & Strauss, B. H. (2019). New elevation data triple estimates of global vulnerability to sea-level rise and coastal flooding. *Nature Communications*, *10*(1). https://doi.org/10.1038/s41467-019-12808-z

Marcy, D., Brooks, W., Draganov, K., Hadley, B., Haynes, C., Herold, N., et al. (2011). New mapping tool and techniques for visualizing sea level rise and coastal flooding impacts. *Solutions to Coastal Disasters 2011 – Proceedings of the 2011 Solutions to Coastal Disasters Conference*. (June), (pp. 474–490). https://doi.org/10.1061/41185(417)42

Milly, P. C. D., Betancourt, J., Falkenmark, M., Hirsch, R. M., Kundzewicz, Z. W., Lettenmaier, D. P., & Stouffer, R. J. (2008). Climate change: Stationarity is dead: Whither water management? *Science*, *319*(5863), 573–574. https://doi.org/10.1126/science.1151915

Nicholls, R. J., Hoozemans, F. M. J., & Marchand, M. (1999). Increasing flood risk and wetland losses due to global sea-level rise: Regional and global analyses. *Global Environmental Change*, *9*(SUPPL), S69–S87. https://doi.org/10.1016/S0959-3780(99)00019-9

NOAA. (2017). Frequently asked questions: Digital coast sea level rise viewer, (January), 1–14. Retrieved from https://coast.noaa.gov/data/digitalcoast/pdf/slr-faq.pdf

Parker, J. K., McIntyre, D., & Noble, R. T. (2010). Characterizing fecal contamination in stormwater runoff in coastal North Carolina, USA. *Water Research*, *44*(14), 4186–4194. https://doi.org/10.1016/j.watres.2010.05.018

Pebesma, E. (2018). Simple features for R: Standardized support for spatial vector data. *The R Journal*, *10*(1), 439. https://doi.org/10.32614/RJ-2018-009

Praharaj, S., Chen, T. D., Zahura, F. T., Behl, M., & Goodall, J. L. (2021). Estimating impacts of recurring flooding on roadway networks: A Norfolk, Virginia case study. *Natural Hazards*, *107*(3), 2363–2387. https://doi.org/10.1007/s11069-020-04427-5

Rogers, B. C., Bertram, N., Gersonius, B., Gunn, A., Löwe, R., Murphy, C., et al. (2020). An interdisciplinary and catchment approach to enhancing urban flood resilience: A Melbourne case. *Philosophical Transactions of the Royal Society A: Mathematical, Physical & Engineering Sciences*, *378*(2168), 20190201. https://doi.org/10.1098/rsta.2019.0201

Rosenzweig, B. R., McPhillips, L., Chang, H., Cheng, C., Welty, C., Matsler, M., et al. (2018). Pluvial flood risk and opportunities for resilience (Vol. *5*). *Wiley Interdisciplinary Reviews: Water (June)*, e1302. https://doi.org/10.1002/wat2.1302

Rotzoll, K., & Fletcher, C. H. (2013). Assessment of groundwater inundation as a consequence of sea-level rise. *Nature Climate Change*, *3*(5), 477–481. https://doi.org/10.1038/nclimate1725

Sadler, J. M., Goodall, J. L., Behl, M., Bowes, B. D., & Morsy, M. M. (2020). Exploring real-time control of stormwater systems for mitigating flood risk due to sea level rise. *Journal of Hydrology*, *583*(January), 124571. https://doi.org/10.1016/j.jhydrol.2020.124571

Schmid, K., Hadley, B., & Waters, K. (2014). Mapping and portraying inundation uncertainty of bathtub-type models. *Journal of Coastal Research*, *30*(3), 548–561. https://doi.org/10.2112/JCOASTRES-D-13-00118.1

Shen, Y., Morsy, M. M., Huxley, C., Tahvildari, N., & Goodall, J. L. (2019). Flood risk assessment and increased resilience for coastal urban watersheds under the combined impact of storm tide and heavy rainfall. *Journal of Hydrology*, *579*(June), 124159. https://doi.org/10.1016/j.jhydrol.2019.124159

Su, X., Liu, T., Beheshti, M., & Prigiobbe, V. (2020). Relationship between infiltration, sewer rehabilitation, and groundwater flooding in coastal urban areas. *Environmental Science and Pollution Research*, *27*(13), 14288–14298. https://doi.org/10.1007/s11356-019-06513-z

Sweet, W. V., Dusek, G., Carbin, G., Marra, J., Marcy, D., & Simon, S. (2020). 2019 state of U.S. high tide flooding with a 2020 outlook (Vol. NOAA Techn). Retrieved from https://www.ncdc.noaa.gov/monitoring-content/sotc/national/2017/may/2016_StateofHighTideFlooding.pdf

Sweet, W. V., Dusek, G., Obeysekera, J., & Marra, J. J. (2018). *Patterns and projections of high tide flooding along the U.S. coastline using a common impact threshold*. NOAA Technical Report NOS CO-OPS 086. (February).

Titus, J. G., Kuo, C. Y., Gibbs, M. J., LaRoche, T. B., Webb, M. K., & Waddell, J. O. (1987). Greenhouse effect, sea level rise, and coastal drainage systems. *Journal of Water Resources Planning and Management*, *113*(2), 2162–2227. https://doi.org/10.1061/(asce)0733-9496(1987)113:2(216)

Wahl, T., Jain, S., Bender, J., Meyers, S. D., & Luther, M. E. (2015). Increasing risk of compound flooding from storm surge and rainfall for major US cities. *Nature Climate Change*, *5*(12), 1093–1097. https://doi.org/10.1038/nclimate2736

Walker, K., & Herman, M. (2021). *tidycensus: Load US census boundary and attribute data as "tidyverse" and "sf"-Ready Data Frames*. Retrieved from https://CRAN.R-project.org/package=tidycensus

Wdowinski, S., Bray, R., Kirtman, B. P., & Wu, Z. (2016). Increasing flooding hazard in coastal communities due to rising sea level: Case study of Miami Beach, Florida. *Ocean & Coastal Management*, *126*(June), 1–8. https://doi.org/10.1016/j.ocecoaman.2016.03.002

Wilby, R. L. (2007). A review of climate change impacts on the built Environment. *Built Environment*, *33*(1), 31–45. https://doi.org/10.2148/benv.33.1.31

Wilby, R. L., & Keenan, R. (2012). Adapting to flood risk under climate change. *Progress in Physical Geography*, *36*, 348–378. https://doi.org/10.1177/0309133312438908

Woodruff, J. D., Irish, J. L., & Camargo, S. J. (2013). Coastal flooding by tropical cyclones and sea-level rise. *Nature*, *504*(7478), 44–52. https://doi.org/10.1038/nature12855

Zervas, C. (2009). Sea level variations of the United States 1854–2006. *Technical Report NOS CO-OPS 053*, *53*(December).